Molecular Pharmacology Fast Forward. Published on January 5, 2017 as DOI: 10.1124/mol.116.107326
This article has not been copyedited and formatted. The final version may differ from this version.

Olefin Isomers of a Triazole Bisphosphonate Synergistically Inhibit Geranylgeranyl Diphosphate Synthase

Cheryl Allen, Sandhya Kortagere, Huaxiang Tong, Robert A. Matthiesen, Joseph I. Metzger, David F. Wiemer, and Sarah A. Holstein

Department of Medicine, Roswell Park Cancer Institute, Buffalo, NY (CA), Department of Microbiology & Immunology, Drexel University, Philadelphia, PA (SK), Penn State Cancer Institute, Hershey, PA (HT), Department of Chemistry, University of Iowa, Iowa City, IA (RAM, JIM, DFW), Department of Internal Medicine, University of Nebraska Medical Center, Omaha, NE (SAH)

Molecular Pharmacology Fast Forward. Published on January 5, 2017 as DOI: 10.1124/mol.116.107326
This article has not been copyedited and formatted. The final version may differ from this version.

Running Title Page

Running Title: Inhibition of geranylgeranyl diphosphate synthase

Corresponding Author:

Sarah A. Holstein, MD, PhD

Department of Internal Medicine

University of Nebraska Medical Center

987680 Nebraska Medical Center, Omaha, NE, 68198-7680

Tel: 402-559-6660

Fax: 402-559-6520

Email: sarah.holstein@unmc.edu

Number of text pages: 23

Number of tables: 1

Number of figures: 8

Number of references: 41

Number of words in Abstract: 243

Number of words in Introduction: 599

Number of words in Discussion: 1039

Abbreviations: BCA, bicinchoninic acid; DMAPP, dimethyl allyl pyrophosphate; FDPS, farnesyl diphosphate synthase; FDP, farnesyl diphosphate; GGDPS, geranylgeranyl diphosphate synthase; GGDP, geranylgeranyl diphosphate; GPP, geranyl pyrophosphate; IPP, isopentenyl pyrophosphate.

Molecular Pharmacology Fast Forward. Published on January 5, 2017 as DOI: 10.1124/mol.116.107326
This article has not been copyedited and formatted. The final version may differ from this version.

Abstract:

The isoprenoid donor for protein geranylgeranylation reactions, geranylgeranyl diphosphate (GGDP), is the product of the enzyme GGDP synthase (GGDPS) which condenses farnesyl diphosphate (FDP) and isopentenyl pyrophosphate. GGDPS inhibition is of interest from a therapeutic perspective for multiple myeloma as we have shown that targeting Rab GTPase geranylgeranylation impairs monoclonal protein trafficking, leading to endoplasmic reticulum stress and apoptosis. We have reported a series of triazole bisphosphonate GGDPS inhibitors of which the most potent was a 3:1 mixture of homogeranyl (HG) and homoneryl (HN) isomers. Here we have determined the activity of the individual olefin isomers. Enzymatic and cellular assays revealed that while HN is approximately 3-fold more potent than HG, HN is not more potent than the original mixture. Studies in which cells were treated with varying concentrations of each isomer alone and in different combinations revealed that the two isomers potentiate the induced-inhibition of protein geranylgeranylation when used in a 3:1 HG:HN combination. A synergistic interaction was observed between the two isomers in the GGDPS enzyme assay. These results suggested that the two isomers bind simultaneously to the enzyme but within different domains. Computational modeling studies revealed that HN is preferred at the FDP site, that HG is preferred at the GGDP site, and that both isomers may bind to the enzyme simultaneously. These studies are the first to report a set of olefin isomers which synergistically inhibit GGDPS thus establishing a new paradigm for the future development of GGDPS inhibitors.

Molecular Pharmacology Fast Forward. Published on January 5, 2017 as DOI: 10.1124/mol.116.107326
This article has not been copyedited and formatted. The final version may differ from this version.

Introduction:

In animals, the isoprenoid biosynthetic pathway begins with the conversion of hydroxymethylglutaryl-coenzyme A (HMG-CoA) to mevalonate by HMG-CoA reductase (HMGR). Mevalonate undergoes phosphorylation and decarboxylation to form isopentenyl pyrophosphate (IPP) which reversibly isomerizes to dimethylallyl pyrophosphate (DMAPP). IPP and DMAPP serve as substrates for farnesyl disphosphate synthase (FDPS) which generates the C_{15} farnesyl diphosphate (FDP) from these C_5 precursors, while FDP and IPP serve as substrates for geranylgeranyl diphosphate synthase (GGDPS), generating the C_{20} geranylgeranyl diphosphate (GGDP). The FDP and GGDP isoprenoid moieties derived from these prenyl synthases play important roles in protein prenylation, a post-translational modification. This modification is necessary for proper intracellular localization and function of proteins such as members of the Ras small GTPase superfamily, many of which are involved in signal transduction pathways. There has been significant focus on the development of inhibitors of the prenyl transferases for pharmacological activity and therapeutic applications (Holstein and Hohl, 2012; Palsuledesai and Distefano, 2015). In the setting of multiple myeloma, we have been focused on the disruption of Rab GTPase geranylgeranylation as a novel therapeutic strategy because our studies have demonstrated that agents which impair Rab geranylgeranylation lead to a disruption of monoclonal protein trafficking, resulting in induction of ER stress and apoptosis (Dykstra et al., 2015; Holstein and Hohl, 2011).

An alternative strategy to the direct inhibition of prenyl transferase activity is to inhibit the prenyl synthases involved in the generation of FDP and GGDP. The nitrogenous bisphosphonates such as zoledronate (Fig. 1) have been widely used in the management of bone disorders, including osteoporosis, metastatic bone disease, and myeloma bone disease. Notably, these agents are specific inhibitors of FDPS (Bergstrom et al., 2000; Dunford et al., 2001) and their anti-resorptive activity is primarily attributed to disruption of protein geranylgeranylation within osteoclasts (Coxon et al., 2000;

Molecular Pharmacology Fast Forward. Published on January 5, 2017 as DOI: 10.1124/mol.116.107326
This article has not been copyedited and formatted. The final version may differ from this version.

Luckman et al., 1998). More recently there has also been interest in the therapeutic potential of GGDPS inhibitors as a more direct way of depleting cellular GGDP levels and thereby disrupting protein geranylgeranylation (Reilly et al., 2016; Wiemer et al., 2011).

Initial efforts in the development of GGDPS inhibitors yielded digeranyl bisphosphonate (Fig. 1) which was found to have an IC_{50} of 260 nM against the enzyme (Shull et al., 2006; Wiemer et al., 2007). Crystallography studies revealed that the V-shaped compound occupied the FDP substrate binding site as well as the GGDP product site within the enzyme's active site (K. M. Chen et al., 2008). Subsequent efforts focused on modifications of the V-shaped motif (Barney et al., 2010; Foust et al., 2016; K. M. Chen et al., 2008; Zhou et al., 2014b). More recently, a series of triazole bisphosphonates were prepared and it was determined that a mixture of geranyl and neryl triazole bisphosphonates (Fig. 1) inhibited GGDPS and that the neryl isomer was approximately 40-fold more potent than the geranyl isomer (IC_{50} 375 nM vs 17 μM) (Zhou et al., 2014a; Zhou et al., 2013). Subsequently a preparation of a homogeranyl/homoneryl triazole bisphosphonate mix (Fig. 1) was identified as the most potent inhibitor of GGDPS described to date with an IC_{50} of 45 nM (Wills et al., 2015). Given the relative activities of the geranyl/neryl isomers, one might predict that the homoneryl isomer would be significantly more potent than the homogeranyl isomer and efforts have therefore been focused on the preparation of the pure isomers (Matthiesen et al., 2016). Here we present our findings for the biological activities of the homogeranyl and homoneryl triazole bisphosphonates and demonstrate that these compounds interact in a synergistic manner to inhibit GGDPS, thus establishing a new paradigm for the development of GGDPS inhibitors.

Molecular Pharmacology Fast Forward. Published on January 5, 2017 as DOI: 10.1124/mol.116.107326
This article has not been copyedited and formatted. The final version may differ from this version.

Materials and Methods:

Reagents: Lovastatin (M2147), geranyl pyrophosphate (G6772), and farnesyl pyrophosphate (F6892) were obtained from Sigma (St. Louis, MO). [^{14}C]-IPP was purchased from American Radiolabeled Chemicals (St. Louis, MO). The pure homogeranyl and homoneryl triazole bisphosphonates (**7** and **8**) and the 3:1 (HG:HN) mixture (**6**) were prepared as previously reported (Matthiesen et al., 2016; Wills et al., 2015). Stock solutions (50 mM) of the triazole bisphosphonate sodium salts were prepared in sterile water and stored at -20 °C. Working dilutions (0.5 μM-50 μM) of the triazole bisphosphonate sodium salts were also prepared in sterile water and stored at -20 °C. Anti-Rap1a (sc-1482), Rab6 (sc-310), and calnexin (sc-23954) antibodies were obtained from Santa Cruz Biotechnology (Santa Cruz, CA). Anti-β-tubulin (T5201) antibody was purchased from Sigma. Secondary HRP-linked antibodies were obtained from Amersham (GE Healthcare Life Sciences, Pittsburgh, PA; (anti-mouse (NA-931) and anti-rabbit (NA934)) or Santa Cruz Biotechnology (anti-goat sc-2020).

Cell culture: Human myeloma cell lines (RPMI-8226, MM.1S) were purchased from American Type Culture Collection (ATCC) (Manassas, VA) and grown in media (per ATCC specifications) which was supplemented with heat-inactivated fetal bovine serum (FBS), glutamine and penicillin-streptomycin at 37 °C and 5% CO_2.

Monoclonal protein quantitation: Cells were incubated in the presence or absence of drugs for specified periods of time. The cells were lysed in RIPA buffer (0.15M NaCl, 1% sodium deoxycholate, 0.1% SDS, 1% Triton (v/v) X-100, 0.05 M Tris HCl, pH 7.4) containing protease and phosphatase inhibitors. Protein content was determined using the BCA method. A human lambda light chain kit (E80-116, Bethyl Laboratories, Montgomery, TX) was used to quantify intracellular monoclonal protein levels.

Immunoblotting: Following incubation with drugs, cells were collected, washed with PBS, and lysed in RIPA buffer as described above. Protein content was determined using the BCA method. Equivalent

Molecular Pharmacology Fast Forward. Published on January 5, 2017 as DOI: 10.1124/mol.116.107326
This article has not been copyedited and formatted. The final version may differ from this version.

amounts of cell lysate were resolved by SDS-PAGE, transferred to polyvinylidene difluoride membrane, probed with the appropriate primary antibodies, and detected using HRP-linked secondary antibodies and Amersham Pharmacia Biotech ECL Western blotting reagents per manufacturer's protocols. For Rab6, cells were lysed with Triton X-114 to generate detergent (membrane) fractions (Wasko et al., 2011).

Measurement of intracellular GGDP levels: Intracellular GGDP levels were measured using the previously reported reversed phase HPLC methodology (Tong et al., 2005). Briefly, isoprenoid pyrophosphates were extracted from cell pellets with extraction solvent (butanol /75 mM ammonium hydroxide/ethanol 1:1.25:2.75) and then dried down with nitrogen gas. The GGDP in the residue was incorporated into fluorescently labeled GCVLL peptide (Biosynthesis, Inc., Lewisville, TX) by recombinant GGTase I, (Jena Biosciences, Jena, Germany) and the prenylated fluorescent peptide was quantified by reversed phase HPLC with fluorescence detection.

FDPS and GGDPS enzyme assays: Recombinant FDPS was kindly provided by Dr. Raymond Hohl, Penn State Cancer Institute. Recombinant GGDPS was obtained from MyBioSource (San Diego, CA). Enzyme assays were performed as previously described (Wills et al., 2015). Compounds were tested in duplicate and three independent experiments were performed.

Modeling: The crystal structure of geranylgeranyl diphosphate synthase in complex with magnesium and BPH-252 was obtained from the protein databank (pdb code: 2Z4Y) (K. M. Chen et al., 2008). The structure was then prepared for docking experiments by removing the ligands, adding hydrogen atoms and refining with energy minimization and 3ns long molecular dynamics simulation using Amber99 force field and charges as adopted in MOE program (ver 10.2). The binding pockets for FDP and GGDP have been well-described in the literature to be overlapping, yet distinct sites (Kavanagh et al., 2006). Three dimensional structures of HG (compound **7**) and HN (compound **8**) were modeled using the ligand

Molecular Pharmacology Fast Forward. Published on January 5, 2017 as DOI: 10.1124/mol.116.107326
This article has not been copyedited and formatted. The final version may differ from this version.

builder module of MOE and refined using AM1 optimization. These compounds were then docked individually to both the FDP and GGDP sites using the GOLD program (Ver 4.1) (Jones et al., 1997). GOLD program uses a genetic algorithm for a conformational search on both the ligand and residues of the binding pocket. Twenty different conformations of HN and HG were sampled independently at the FDP and GGDP sites and the docked complexes were ranked using Goldscore and Chemscore scoring schemes (Jones et al., 1997; Verdonk et al., 2003). The probability of binding of HN and HG at the FDP or GGDP sites were determined by comparing the binding energy of the complexes at each site. Further, the best-ranking of HN and HG conformations were simultaneously docked using the MOE program and the complex was minimized.

Statistics: ANOVA testing using the Holm correction for multiple comparisons was used to calculate statistical significance (Aickin and Gensler, 1996). Enzyme assay IC_{50}'s and combination indices were determined via CalcuSyn software (Biosoft, Cambridge, UK). The software analyzes drug interactions based on the method of Chou and Talalay (Chou and Talalay, 1984).

Results

*Homoneryl triazole bisphosphonate (**8**) more potently disrupts cellular geranylgeranylation than homogeranyl triazole bisphosphonate (**7**).* Cell culture studies were performed to determine the relative potencies of the HG and HN isomers in disrupting geranylgeranylation. We have previously demonstrated that inhibition of Rab geranylgeranylation results in accumulation of intracellular monoclonal protein levels in myeloma cells and that changes in this protein level can be used as a surrogate marker for disruption of geranylgeranylation (Holstein and Hohl, 2011; Wills et al., 2015). An ELISA analysis of lambda light chain levels following treatment with either HG or HN in MM cells (RPMI-8226 (Fig. 2A) and MM.1S (Supplemental Figure 1)) revealed that the HN isomer more potently induces

Molecular Pharmacology Fast Forward. Published on January 5, 2017 as DOI: 10.1124/mol.116.107326
This article has not been copyedited and formatted. The final version may differ from this version.

accumulation of intracellular light chain as compared to the HG isomer. This disruption in protein geranylgeranylation was confirmed with immunoblot analysis of Rap1a using a primary antibody that is specific for unmodified protein. As shown in figure 2B, HN more potently induces the accumulation of unmodified Rap1a as compared to the HG isomer. To more directly assess the disruption of Rab geranylgeranylation, Triton X-114 lysis was performed on RPMI-8226 cells treated with either isomer and immunoblot analysis of the detergent fraction (membrane-bound fraction) was performed (Fig. 2C). While a decrease in modified Rab6 was observed following treatment with 50 nM HN, a 3-fold higher concentration (150 nM) of HG was required to exert similar effects.

Homoneryl triazole bisphosphonate more potently depletes cellular GGDP levels than homogeranyl triazole bisphosphonate. The effects of the isomers on intracellular GGDP levels were assessed. Consistent with the geranylgeranylation studies, the HN isomer is more potent than the HG isomer in depleting cellular GGDP levels (Fig. 3). In aggregate, these studies suggested that the HN isomer was 2-3 times more potent than the HG isomer.

Homoneryl triazole bisphosphonate is a potent and specific inhibitor of GGDPS. In vitro enzyme assays were performed in order to directly assess the ability of each isomer to inhibit GGDPS. As shown in Table 1, the HN isomer was found to be more potent than HG, confirming the results of the cellular assays. Neither isomer potently inhibited the related enzyme FDPS, demonstrating specificity towards GGDPS of approximately 365:1.

Lovastatin potentiates the effects of the GGDPS inhibitors. Lovastatin, as a representative HMG-CoA reductase inhibitor, globally disrupts prenylation as a consequence of depletion of mevalonate and longer chain isoprenoids. Typically, micromolar concentrations of this drug are required to exert this effect, and therefore this is not considered to be clinically relevant as standard statin dosing yields plasma levels of approximately 0.1 μM (Pan et al., 1990). In these assays, cells were incubated in the

Molecular Pharmacology Fast Forward. Published on January 5, 2017 as DOI: 10.1124/mol.116.107326
This article has not been copyedited and formatted. The final version may differ from this version.

presence or absence of sub-maximal concentrations of either HG or HN in combination with 0.1 μM lovastatin. As shown in figure 4, submicromolar lovastatin alone did not disrupt protein geranylgeranylation as evidenced by the lack of changes in intracellular light chain levels (Fig. 4A) or appearance of unmodified Rap1a (Fig. 4B). However, when cells were co-incubated with lovastatin and either HG or HN there was an increase in both intracellular light chain levels and unmodified Rap1a levels compared to HG or HN alone.

The combination of the two isomers more potently disrupts cellular geranylgeranylation than either isomer alone. Based on previous work with the geranyl and neryl triazole bisphosphonates, which demonstrated that the neryl isomer was more potent than either the geranyl isomer or the originally reported mixture of the two isomers (Zhou et al., 2014a), it was hypothesized that the HN isomer would not only be more potent than the HG isomer, but would also be more potent than the original mixture **6**. The *in vitro* enzyme assay results (Table 1) confirmed that HN is more potent than HG but not more potent than the mixture **6**. Studies were therefore performed to more directly compare the cellular activity of the mixture to the pure HN isomer. The activity of the mixture **6** and HN was very similar across a concentration range of 10-50 nM (Fig.5 and Supplemental Figure 2). As the original mixture is a 3:1 ratio in favor of the less potent isomer (3:1 HG:HN) (Wills et al., 2015), these results suggested that the two isomers might interact with each other. Therefore, studies were performed in which cells were incubated with varying combinations of HN and HG. Marked increases in both intracellular light chains and unmodified Rap1a levels were observed when cells were treated with a 3:1 ratio of HG:HN (figure 6). Conversely, no enhancement in activity was observed when cells were treated with a 1:3 ratio of HG:HN (Supplemental Figure 3). Combinations involving a 1:1 ratio showed some enhancement in activity, but less so than with the 3:1 mixture (Supplemental Figure 4).

Molecular Pharmacology Fast Forward. Published on January 5, 2017 as DOI: 10.1124/mol.116.107326
This article has not been copyedited and formatted. The final version may differ from this version.

Homogeranyl and homoneryl triazole bisphosphonates synergistically inhibit GGDPS. To determine whether the results of the cell culture combination studies are a consequence of interaction of the two isomers at the level of the enzyme, *in vitro* enzyme studies were performed. As shown in figure 7, the combination of the two isomers (3:1 HG:HN) inhibited GGDPS activity more potently than either isomer alone. Isobologram analysis revealed a synergistic interaction with combination indices (CI) of three independent experiments less than one (CI of 0.57 $\pm$ 0.28 for EC_{50}).

Modeling of HG and HN in the GGDPS active site. Molecular docking studies of HN and HG to the FDP and GGDP sites suggested that the HN and HG had preferential docking probabilities to the two sites (Fig. 8). The HN isomer favored binding at the FDP site with a high probability and 75% of the sampled conformations had a docking score of >62 at the FDP site. Similarly, HG had a higher probability of binding to the GGDP site and 64% of sampled conformations had a docking score of >72 at the GGDP site. Interactions of HN at the FDP site were mediated by hydrogen-bonded interactions between the ligand and arginine residues 44, 89, and 90. In addition, histidine 73, tyrosine 210 and several hydrophobic residues contributed to the high affinity interactions of HN. The binding of HG to the GGDP site was mediated by an arene-H interaction between the triazole and lysine 238 as well as several hydrogen bonding partners including tyrosine 210, glutamine 147, threonine 175, and lysine 174. Several hydrophobic interactions also appear to stabilize the ligand in this binding pocket. Further, docking studies also suggested that both HN and HG could bind simultaneously to these two sites with a potential for synergistic interactions (Fig. 8).

Discussion:

Pharmacological inhibition of GGDPS, as opposed to other enzymes in the isoprenoid biosynthetic pathway, results in disruption of geranylgeranylation while leaving the remainder of the pathway (including cholesterol synthesis and farnesylation) intact. Not only has our work demonstrated

Molecular Pharmacology Fast Forward. Published on January 5, 2017 as DOI: 10.1124/mol.116.107326
This article has not been copyedited and formatted. The final version may differ from this version.

potential for GGDPS inhibitors as anti-myeloma agents (Dykstra et al., 2015; Holstein and Hohl, 2011; Zhou et al., 2014a), but there has also been interest in the use of GGDPS inhibitors as anti-cancer agents for solid tumors models (Reilly et al., 2016) and in non-malignant conditions such as pulmonary fibrosis (Osborn-Heaford et al., 2015).

Previous efforts to develop GGDPS inhibitors have focused in large part on branched compounds, including V-shaped inhibitors such as DGBP and its analogues as well as more recently U-shaped inhibitors (Barney et al., 2010; Foust et al., 2016; K. M. Chen et al., 2008; Wiemer et al., 2007; Zhou et al., 2014b). Prior crystallography studies demonstrated that the V-shaped compounds can occupy both the FDP and the GGDP sites (K. M. Chen et al., 2008). Based on the activity of the branched inhibitors, the activity of the mono-alkylated triazole bisphosphonates as GGDPS inhibitors was unexpected (Zhou et al., 2014a). Dialkylated triazoles bisphosphonates, while maintaining activity as GGDPS inhibitors, were not more potent than the monoalkylated versions (Wills et al., 2015)(unpublished data), suggesting that the triazole moiety plays an important role in modulating the interaction between the inhibitor and the enzyme.

There have been conflicting reports regarding the manner in which GGDPS monomers associate in solution. Kuzuguchi et al., reported a molecular weight of 280-kDa, which would correlate with GGDPS being an octomer (each monomer has a molecular weight of 34.96 kDa) (Kuzuguchi et al., 1999). Work done by Kavanagh et al., suggested that based on molecular weight, 5-6 monomers are associated per molecule (molecular weight 193 kDa) in solution (Kavanagh et al., 2006). Sagami et al., reported that GGDPS from bovine brain is a homooligomer (150-195 kDa) with a monomer molecular mass of 37.5 kDa (Sagami et al., 1994) while Miyagi et al., reported that the active form of GGDPS in solution is an octomer and that hexamer and dimer forms could be converted to the octamer form by treating with dithiothreitol (Miyagi et al., 2007). Crystallography studies by Kavanagh et al., revealed a hexameric

Molecular Pharmacology Fast Forward. Published on January 5, 2017 as DOI: 10.1124/mol.116.107326
This article has not been copyedited and formatted. The final version may differ from this version.

organization of three dimers in which each of the six protein chains is associated with two Mg^{2+} ions and one GGDP molecule (Kavanagh et al., 2006).

Based on the computational modeling studies, both HG and HN can simultaneously bind to distinct but overlapping sites within the enzyme (HG with preference for the GGDP site and HN with preference for the FDP site) (Fig. 8). These preliminary results suggest synergistic interactions between HN and HG molecules but do not explain the observed 3:1 stoichiometry observed in enzymatic assays. That the highest degree of synergy is observed when the two isomers are in a 3:1 HG:HN ratio, may be related to the oligomeric nature of the enzyme in solution. It can be hypothesized that, for example, binding of one HG molecule to the product site of one GGDPS monomer could change the conformation of the other monomers in the complex such that the affinity of subsequent HG or HN binding is altered. Future crystallography studies with the enzyme in complex with HG and/or HN will be important to more clearly define the manner in which the two isomers bind and interact with the enzyme.

Many clinically used agents are chiral and have been used as racemic mixtures. There is precedence for the enantiomers to have different relative activities against the same target, as well as different pharmacokinetic properties (Lu, 2007). For example, while the binding of the (*S*)-enantiomer of the myeloma drug thalidomide to cereblon is favored over the binding of the (*R*)-enantiomer (Fischer et al., 2014), the two enantiomers have different clearances such that the blood concentration of the (*R*)-enantiomer is higher (Eriksson et al., 2001; Eriksson et al., 1995). The anti-depressant bupropion is racemic as is its major metabolite hydroxybupropion, however, the (*2S, 3S*)-hydroxy isomer is significantly more potent than the (*2S, 3R*) hydroxy isomer (Damaj et al., 2004). In a recent report investigating novel allosteric modulators of dopamine receptors, which are of interest for the treatment of Parkinson's disease, it was found that the (*R*)-isomer acted as a positive allosteric modulator while the (*S*)-isomer had negative allosteric modulator properties (Wood et al., 2016). Examples of enantiomers

Molecular Pharmacology Fast Forward. Published on January 5, 2017 as DOI: 10.1124/mol.116.107326
This article has not been copyedited and formatted. The final version may differ from this version.

having synergistic properties have also been reported, including enantiomeric iminosugars (Jenkinson et al., 2011) and methadone (Silverman et al., 2009). To our knowledge, the present study is the first reported case of olefin stereoisomers having synergistic activity against an enzyme. Future studies will determine whether these isomers have different pharmacokinetic properties.

In contrast to FDPS, no substrate inhibition of GGDPS by IPP has been observed (Kavanagh et al., 2006). However, there is evidence that GGDP is a competitive inhibitor with respect to FDP (Kavanagh et al., 2006; Sagami et al., 1994), thus providing a mechanism by which the enzyme regulates GGDP production. This feature predicts relatively stable levels of GGDP under conditions of upstream substrate depletion. Submicromolar levels of lovastatin, which are sufficient to alter isoprenoid levels and inhibit cholesterol biosynthesis but insufficient to disrupt protein geranylgeranylation (Sinensky et al., 1990), potentiate the activity of low concentrations of the HG/HN isomers (Fig. 4). These findings are consistent with enhanced enzyme inhibition as a consequence of depletion of the substrates as well as by increasing the access of the inhibitors to the GGDP binding site by depleting available GGDP. From a therapeutic perspective, this finding is relevant because it suggests that the clinical efficacy of HG/HN could be enhanced by the co-administration of standard doses of statins and therefore the toxicities associated with high doses of statins (Holstein et al., 2006; Thibault et al., 1996) could be avoided.

In conclusion, the mixture 6 is the most potent GGDPS inhibitor identified to date. We have now demonstrated that while the HN isomer is more potent an inhibitor than the HG isomer, notably, the two isomers in combination behave in a synergistic manner. Future studies will focus on further defining the precise mechanisms by which these isomers interact with GGDPS and determining the preclinical activity of these novel GGDPS inhibitors.

Molecular Pharmacology Fast Forward. Published on January 5, 2017 as DOI: 10.1124/mol.116.107326
This article has not been copyedited and formatted. The final version may differ from this version.

Acknowledgements: We thank Staci Haney, PhD, for her assistance with the statistical analysis.

Authorship Contributions:

Participated in research design: Wiemer, Holstein

Conducted experiments: Allen, Kortagere, Tong, Holstein

Contributed new reagents or analytic tools: Matthiesen, Metzger, Wiemer

Performed data analysis: Allen, Kortagere, Tong, Holstein

Wrote or contributed to the writing of the manuscript: Kortagere, Wiemer, Holstein

Molecular Pharmacology Fast Forward. Published on January 5, 2017 as DOI: 10.1124/mol.116.107326
This article has not been copyedited and formatted. The final version may differ from this version.

References

Aickin M and Gensler H (1996) Adjusting for multiple testing when reporting research results: the Bonferroni vs Holm methods. *Am J Public Health* **86**(5): 726-728.

Barney RJ, Wasko BM, Dudakovic A, Hohl RJ and Wiemer DF (2010) Synthesis and biological evaluation of a series of aromatic bisphosphonates. *Bioorg Med Chem* **18**(20): 7212-7220.

Bergstrom JD, Bostedor RG, Masarachia PJ, Reszka AA and Rodan G (2000) Alendronate is a specific, nanomolar inhibitor of farnesyl diphosphate synthase. *Arch Biochem Biophys* **373**(1): 231-241.

Chou TC and Talalay P (1984) Quantitative analysis of dose-effect relationships: the combined effects of multiple drugs or enzyme inhibitors. *Adv Enzyme Regul* **22**: 27-55.

Coxon FP, Helfrich MH, Van't Hof R, Sebti S, Ralston SH, Hamilton A and Rogers MJ (2000) Protein geranylgeranylation is required for osteoclast formation, function, and survival: inhibition by bisphosphonates and GGTI-298. *J Bone Miner Res* **15**(8): 1467-1476.

Damaj MI, Carroll FI, Eaton JB, Navarro HA, Blough BE, Mirza S, Lukas RJ and Martin BR (2004) Enantioselective effects of hydroxy metabolites of bupropion on behavior and on function of monoamine transporters and nicotinic receptors. *Mol Pharmacol* **66**(3): 675-682.

Dunford JE, Thompson K, Coxon FP, Luckman SP, Hahn FM, Poulter CD, Ebetino FH and Rogers MJ (2001) Structure-activity relationships for inhibition of farnesyl diphosphate synthase in vitro and inhibition of bone resorption in vivo by nitrogen-containing bisphosphonates. *J Pharmacol Exp Ther* **296**(2): 235-242.

Dykstra KM, Allen C, Born EJ, Tong H and Holstein SA (2015) Mechanisms for autophagy modulation by isoprenoid biosynthetic pathway inhibitors in multiple myeloma cells. *Oncotarget* **6**(39): 41535-41549.

Eriksson T, Bjorkman S and Hoglund P (2001) Clinical pharmacology of thalidomide. *Eur J Clin Pharmacol* **57**(5): 365-376.

Eriksson T, Bjorkman S, Roth B, Fyge A and Hoglund P (1995) Stereospecific determination, chiral inversion in vitro and pharmacokinetics in humans of the enantiomers of thalidomide. *Chirality* **7**(1): 44-52.

Fischer ES, Bohm K, Lydeard JR, Yang H, Stadler MB, Cavadini S, Nagel J, Serluca F, Acker V, Lingaraju GM, Tichkule RB, Schebesta M, Forrester WC, Schirle M, Hassiepen U, Ottl J, Hild M, Beckwith RE, Harper JW, Jenkins JL and Thoma NH (2014) Structure of the DDB1-CRBN E3 ubiquitin ligase in complex with thalidomide. *Nature* **512**(7512): 49-53.

Foust BJ, Allen C, Holstein SA and Wiemer DF (2016) A new motif for inhibitors of geranylgeranyl diphosphate synthase. *Bioorg Med Chem* **24**(16): 3734-3741.

Holstein SA and Hohl RJ (2011) Isoprenoid biosynthetic pathway inhibition disrupts monoclonal protein secretion and induces the unfolded protein response pathway in multiple myeloma cells. *Leuk Res* **35**(4): 551-559.

Holstein SA and Hohl RJ (2012) Is there a future for prenyltransferase inhibitors in cancer therapy? *Curr Opin Pharmacol* **12**(6): 704-709.

Holstein SA, Knapp HR, Clamon GH, Murry DJ and Hohl RJ (2006) Pharmacodynamic effects of high dose lovastatin in subjects with advanced malignancies. *Cancer Chemother Pharmacol* **57**(2): 155-164.

Jenkinson SF, Fleet GW, Nash RJ, Koike Y, Adachi I, Yoshihara A, Morimoto K, Izumori K and Kato A (2011) Looking-glass synergistic pharmacological chaperones: DGJ and L-DGJ from the enantiomers of tagatose. *Org Lett* **13**(15): 4064-4067.

Jones G, Willett P, Glen RC, Leach AR and Taylor R (1997) Development and validation of a genetic algorithm for flexible docking. *J Mol Biol* **267**(3): 727-748.

K. M. Chen C, Hudock MP, Zhang Y, Guo RT, Cao R, No JH, Liang PH, Ko TP, Chang TH, Chang SC, Song Y, Axelson J, Kumar A, Wang AH and Oldfield E (2008) Inhibition of geranylgeranyl diphosphate

synthase by bisphosphonates: a crystallographic and computational investigation. *J Med Chem* **51**(18): 5594-5607.

Kavanagh KL, Dunford JE, Bunkoczi G, Russell RG and Oppermann U (2006) The crystal structure of human geranylgeranyl pyrophosphate synthase reveals a novel hexameric arrangement and inhibitory product binding. *J Biol Chem* **281**(31): 22004-22012.

Kuzuguchi T, Morita Y, Sagami I, Sagami H and Ogura K (1999) Human geranylgeranyl diphosphate synthase. cDNA cloning and expression. *J Biol Chem* **274**(9): 5888-5894.

Lu H (2007) Stereoselectivity in drug metabolism. *Expert Opin Drug Metab Toxicol* **3**(2): 149-158.

Luckman SP, Coxon FP, Ebetino FH, Russell RG and Rogers MJ (1998) Heterocycle-containing bisphosphonates cause apoptosis and inhibit bone resorption by preventing protein prenylation: evidence from structure-activity relationships in J774 macrophages. *J Bone Miner Res* **13**(11): 1668-1678.

Matthiesen RA, Wills VS, Metzger JI, Holstein SA and Wiemer DF (2016) Stereoselective Synthesis of Homoneryl and Homogeranyl Triazole Bisphosphonates. *J Org Chem* **81**(19): 9438-9442.

Miyagi Y, Matsumura Y and Sagami H (2007) Human geranylgeranyl diphosphate synthase is an octamer in solution. *J Biochem* **142**(3): 377-381.

Osborn-Heaford HL, Murthy S, Gu L, Larson-Casey JL, Ryan AJ, Shi L, Glogauer M, Neighbors JD, Hohl R and Brent Carter A (2015) Targeting the isoprenoid pathway to abrogate progression of pulmonary fibrosis. *Free Radic Biol Med* **86**: 47-56.

Palsuledesai CC and Distefano MD (2015) Protein prenylation: enzymes, therapeutics, and biotechnology applications. *ACS Chem Biol* **10**(1): 51-62.

Pan HY, DeVault AR, Wang-Iverson D, Ivashkiv E, Swanson BN and Sugerman AA (1990) Comparative pharmacokinetics and pharmacodynamics of pravastatin and lovastatin. *J Clin Pharmacol* **30**(12): 1128-1135.

Reilly JE, Neighbors JD and Hohl RJ (2016) Targeting protein geranylgeranylation slows tumor development in a murine model of prostate cancer metastasis. *Cancer Biol Ther*: 0.

Sagami H, Morita Y and Ogura K (1994) Purification and properties of geranylgeranyl-diphosphate synthase from bovine brain. *J Biol Chem* **269**(32): 20561-20566.

Shull LW, Wiemer AJ, Hohl RJ and Wiemer DF (2006) Synthesis and biological activity of isoprenoid bisphosphonates. *Bioorg Med Chem* **14**(12): 4130-4136.

Silverman DA, Nettleton RT, Spencer KB, Wallisch M and Olsen GD (2009) S-Methadone augments R-methadone induced respiratory depression in the neonatal guinea pig. *Respir Physiol Neurobiol* **169**(3): 252-261.

Sinensky M, Beck LA, Leonard S and Evans R (1990) Differential inhibitory effects of lovastatin on protein isoprenylation and sterol synthesis. *J Biol Chem* **265**(32): 19937-19941.

Thibault A, Samid D, Tompkins AC, Figg WD, Cooper MR, Hohl RJ, Trepel J, Liang B, Patronas N, Venzon DJ, Reed E and Myers CE (1996) Phase I study of lovastatin, an inhibitor of the mevalonate pathway, in patients with cancer. *Clin Cancer Res* **2**(3): 483-491.

Tong H, Holstein SA and Hohl RJ (2005) Simultaneous determination of farnesyl and geranylgeranyl pyrophosphate levels in cultured cells. *Analytical Biochemistry* **336**: 51-59.

Verdonk ML, Cole JC, Hartshorn MJ, Murray CW and Taylor RD (2003) Improved protein-ligand docking using GOLD. *Proteins* **52**(4): 609-623.

Wasko BM, Dudakovic A and Hohl RJ (2011) Bisphosphonates induce autophagy by depleting geranylgeranyl diphosphate. *J Pharmacol Exp Ther* **337**(2): 540-546.

Wiemer AJ, Tong H, Swanson KM and Hohl RJ (2007) Digeranyl bisphosphonate inhibits geranylgeranyl pyrophosphate synthase. *Biochem Biophys Res Commun* **353**(4): 921-925.

Wiemer AJ, Wiemer DF and Hohl RJ (2011) Geranylgeranyl diphosphate synthase: an emerging therapeutic target. *Clin Pharmacol Ther* **90**(6): 804-812.

Wills VS, Allen C, Holstein SA and Wiemer DF (2015) Potent Triazole Bisphosphonate Inhibitor of Geranylgeranyl Diphosphate Synthase. *ACS Med Chem Lett* **6**(12): 1195-1198.

Wood M, Ates A, Andre VM, Michel A, Barnaby R and Gillard M (2016) In Vitro and In Vivo Identification of Novel Positive Allosteric Modulators of the Human Dopamine D2 and D3 Receptor. *Mol Pharmacol* **89**(2): 303-312.

Zhou X, Ferree SD, Wills VS, Born EJ, Tong H, Wiemer DF and Holstein SA (2014a) Geranyl and neryl triazole bisphosphonates as inhibitors of geranylgeranyl diphosphate synthase. *Bioorg Med Chem* **22**(9): 2791-2798.

Zhou X, Hartman SV, Born EJ, Smits JP, Holstein SA and Wiemer DF (2013) Triazole-based inhibitors of geranylgeranyltransferase II. *Bioorg Med Chem Lett* **23**(3): 764-766.

Zhou X, Reilly JE, Loerch KA, Hohl RJ and Wiemer DF (2014b) Synthesis of isoprenoid bisphosphonate ethers through C-P bond formations: Potential inhibitors of geranylgeranyl diphosphate synthase. *Beilstein J Org Chem* **10**: 1645-1650.

Molecular Pharmacology Fast Forward. Published on January 5, 2017 as DOI: 10.1124/mol.116.107326
This article has not been copyedited and formatted. The final version may differ from this version.

Footnotes:

This project was supported by the National Institutes of Health [R01 CA172070], the American Society of Hematology and the Roy J. Carver Charitable Trust.

Portions of these data have been presented as abstracts at the following meetings:

American Society of Hematology Annual Meeting 2016

Reprint requests should be sent to:

Sarah A. Holstein, MD, PhD

University of Nebraska Medical Center

987680 Nebraska Medical Center

Omaha, NE 68198-7680

Molecular Pharmacology Fast Forward. Published on January 5, 2017 as DOI: 10.1124/mol.116.107326
This article has not been copyedited and formatted. The final version may differ from this version.

Figure Legends

Figure 1. Inhibitors of FDPS and GGDPS. Chemical structures of FDPS and GGDPS inhibitors. IC_{50} values are presented for previously published GGDPS inhibitors.

Figure 2. HN more potently disrupts protein geranylgeranylation than HG. RPMI-8226 and MM.1S cells were incubated for 48 hours in the presence or absence of varying concentrations of HG and HN (10-200 nM). A) RPMI-8226 intracellular lambda light chain levels were measured via ELISA. Data are expressed as a percentage of control (mean ± standard deviation of 3 independent experiments). *Denotes statistical significance as determined by ANOVA testing with the Holm correction for multiple comparisons comparing treated cells to control cells. B) Immunoblot analysis of whole cell lysate (RPMI-8826 (*R*), MM.1S (*M*)) for Rap1a (antibody detects only unmodified protein) and β-tubulin (loading control) was performed. Lovastatin (*Lov*, 10 μM) was included as a positive control. Blots are representative of at least three independent experiments. C) RPMI-8226 cells were incubated for 48 hours in the presence or absence of lovastatin (*Lov*, 10 μM), HG (50 or 150 nM), or HN (50 or 150 nM). Triton X-114 lysis was performed with immunoblot analysis of Rab6 (representative Rab GTPase) and calnexin (loading control). Densitometric analysis of Rab6 (normalized to calnexin) for the treated cells normalized to untreated (control) cells is shown. Data are displayed as mean ± standard deviation (n=3 independent experiments). *Denotes statistical significance as determined by ANOVA testing with the Holm correction for multiple comparisons comparing treated cells to control cells.

Figure 3. Effects of HG, HN, and the mixture 6 on intracellular GGDP levels. RPMI-8226 cells were treated for 48 hours with varying concentrations (50-200 nM) of HG, HN, or the mixture **6**. GGDP was extracted and quantified as described in the Materials and Methods section. Data are expressed as a percentage of control (mean ± standard deviation of two independent experiments). *Denotes

statistical significance as determined by ANOVA testing with the Holm correction for multiple comparisons comparing treated cells to control cells.

Figure 4. Lovastatin enhances the effects of HG and HN. RPMI-8226 cells were incubated for 48 hours in the presence or absence of lovastatin (*Lov*, 0.1 μM) and HG (50-100 nM) or HN (25-50 nM). A) Intracellular lambda light chain levels were measured via ELISA. Data are expressed as a percentage of control (mean ± standard deviation of 3 independent experiments). *Denotes statistical significance as determined by ANOVA testing with the Holm correction for multiple comparisons comparing treatments with and without lovastatin. B) Immunoblot analysis of whole cell lysate for Rap1a (antibody detects only unmodified protein) and β-tubulin (loading control) was performed. Blots are representative of at least three independent experiments.

Figure 5. The mixture 6 and HN have similar cellular activity. RPMI-8226 and MM.1S cells were incubated for 48 hours in the presence or absence of varying concentrations (10-50 nM) of mixture **6** (*Mix 6)* and HN. A) RPMI-8226 intracellular lambda light chain levels were measured via ELISA. Data are expressed as a percentage of control (mean ± standard deviation of 3 independent experiments). *Denotes statistical significance as determined by ANOVA testing with the Holm correction for multiple comparisons comparing treated cells to control cells. B) Immunoblot analysis of whole cell lysate (RPMI-8826 (*R*), MM.1S (*M*)) for Rap1a (antibody detects only unmodified protein) and β-tubulin (loading control) was performed. Lovastatin (*Lov*, 10 μM) was included as a positive control. Blots are representative of three independent experiments.

Figure 6. The combination of HG and HN in a 3:1 ratio enhances disruption of protein geranylgeranylation. RPMI-8226 and MM.1S cells were incubated for 48 hours in the presence or absence of varying concentrations (nM) of HG, HN, or the combination of the two isomers. A) Intracellular lambda light chain levels were measured via ELISA. Data are expressed as a percentage of

control (mean ± standard deviation of 3 independent experiments). *Denotes statistical significance as determined by ANOVA testing with the Holm correction for multiple comparisons comparing treated cells to control cells. B) Immunoblot analysis of whole cell lysate (RPMI-8826 (*R*), MM.1S (*M*)) for Rap1a and β-tubulin (loading control) was performed. Lovastatin (*Lov*, 10 μM) was included as a positive control. Blots are representative of three independent experiments.

Figure 7 HG and HN inhibit GGDPS in a synergistic manner. Recombinant GGDPS was incubated with substrates ([^{14}C]-IPP and FDP) in the presence or absence of inhibitors (HG, HN, or the two isomers in combination (3:1)) and GGDPS activity was determined via quantification of [^{14}C]-GGDP. Data are expressed as mean ± standard deviation (n=2) and are representative of three independent experiments.

Figure 8. Modeling studies reveal preferential binding of HN to the FDP site and HG to the GGDP site and their ability to simultaneously bind GGDPS. A) HN and HG docked to FDP and GGDP sites of GGDPS. The protein is represented in cartoon format with cylinders representing helices and colored orange. HN and HG are represented as licorice sticks and colored atom type (Carbon = cyan, Nitrogen = blue, Oxygen = red, Phosphorus = yellow and Sodium = purple). The position of the Mg^{2+} ion is shown as a green oval. B) Two-dimensional representations of HN (left) and HG (right) docked to FDP and GGDP binding pockets generated using ligX module of MOE program. The schematic legend below describes the nature of the interactions.

Molecular Pharmacology Fast Forward. Published on January 5, 2017 as DOI: 10.1124/mol.116.107326
This article has not been copyedited and formatted. The final version may differ from this version.

Table 1. Inhibitory activities of the homogeranyl and homoneryl triazole bisphosphonates against GGDPS and FDPS.

	GGDPS IC_{50} (nM)	FDPS IC_{50} (μM)
Homogeranyl **7**	173.3 ± 12.7	49.6 ± 8.2
Homoneryl **8**	74.9 ± 6.2	33.3 ± 5.6
Mixture **6** (Wills et al., 2015)	44.7 ± 16.1	28.0 ± 5.0

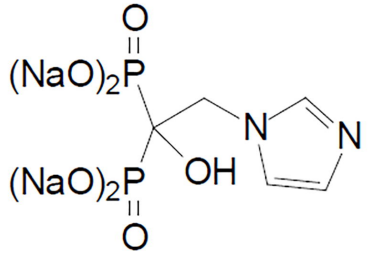

1 (zoledronate)

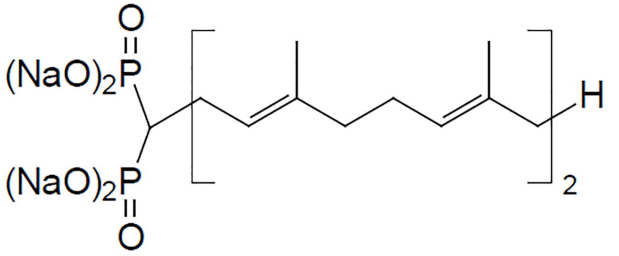

2 (DGBP)

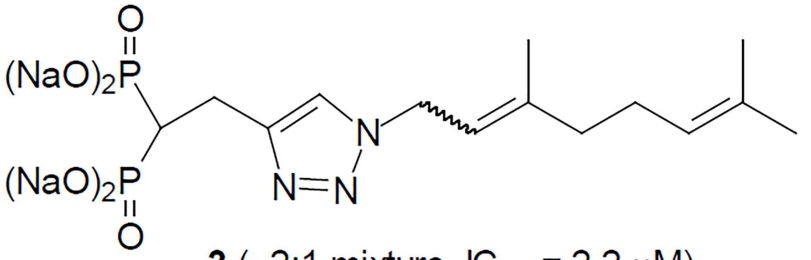

3 (~2:1 mixture, IC_{50} = 2.2 μM)

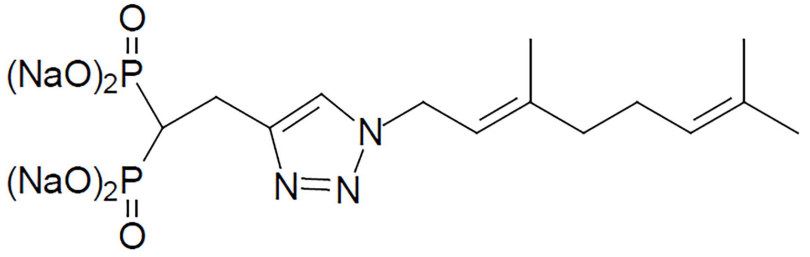

4 (geranyl, IC_{50} = 17 μM)

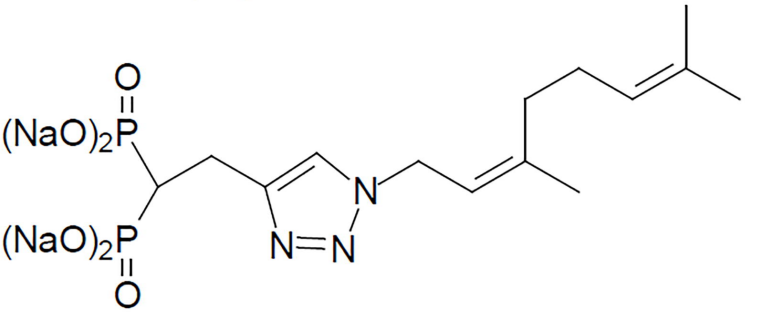

5 (neryl, IC_{50} = 0.38 μM)

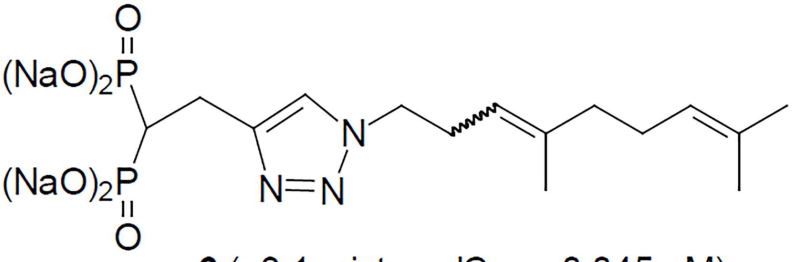

6 (~3:1 mixture, IC_{50} = 0.045 μM)

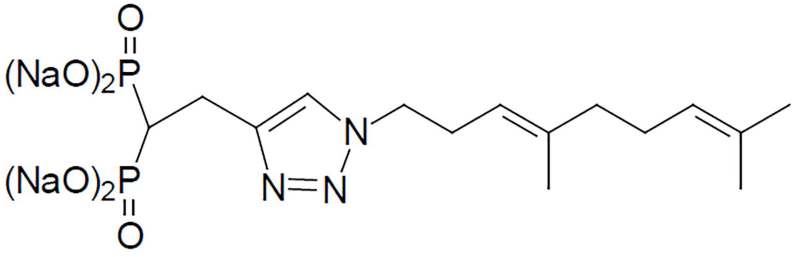

7 (homogeranyl)

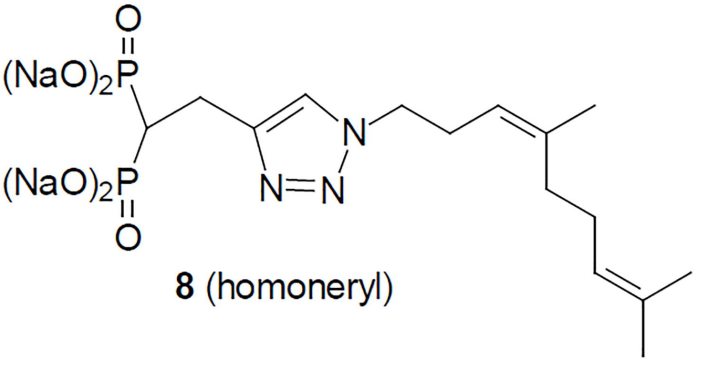

8 (homoneryl)

Figure 1

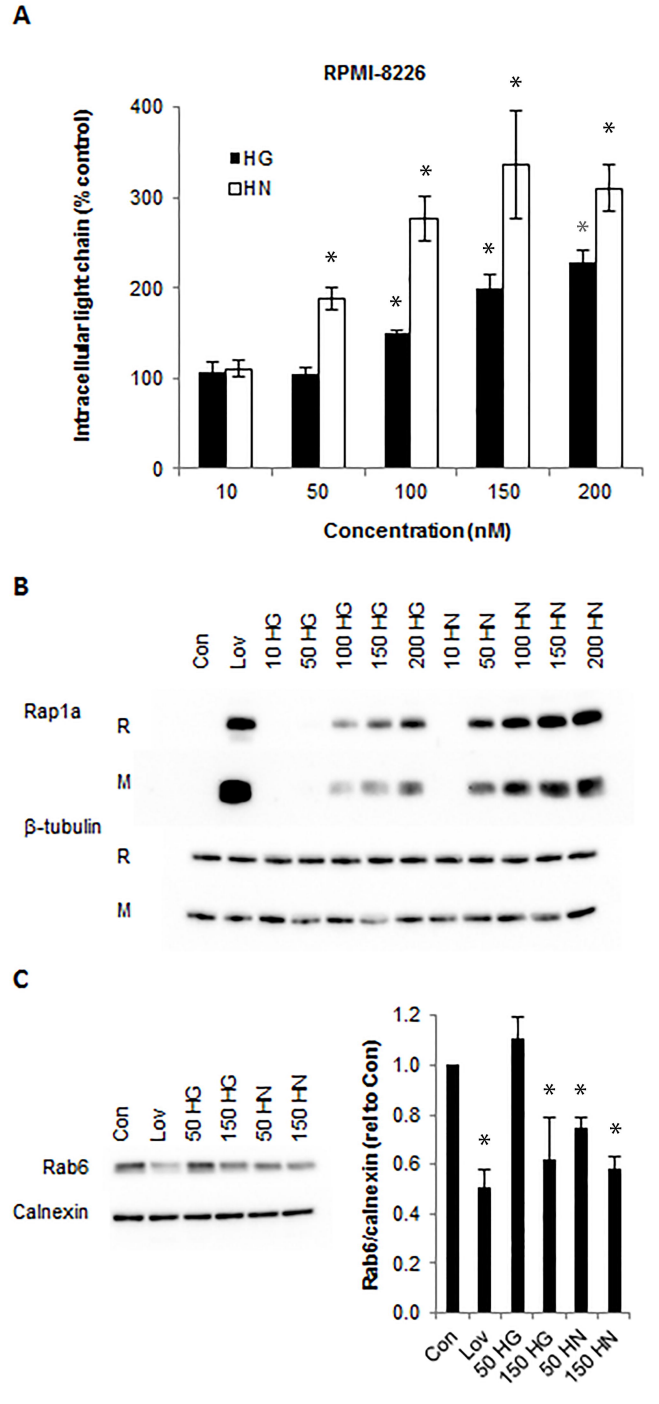
A
RPMI-8226
Intracellular light chain (% control)
HG
HN
400
300
200
100
0
10
50
100
150
200
Concentration (nM)
B
Con
Lov
10 HG
50 HG
100 HG
150 HG
200 HG
10 HN
50 HN
100 HN
150 HN
200 HN
Rap1a
R
M
β-tubulin
R
M
C
Con
Lov
50 HG
150 HG
50 HN
150 HN
Rab6
Calnexin
Rab6/calnexin (rel to Con)
1.2
1.0
0.8
0.6
0.4
0.2
0.0
Con
Lov
50 HG
150 HG
50 HN
150 HN

Figure 2

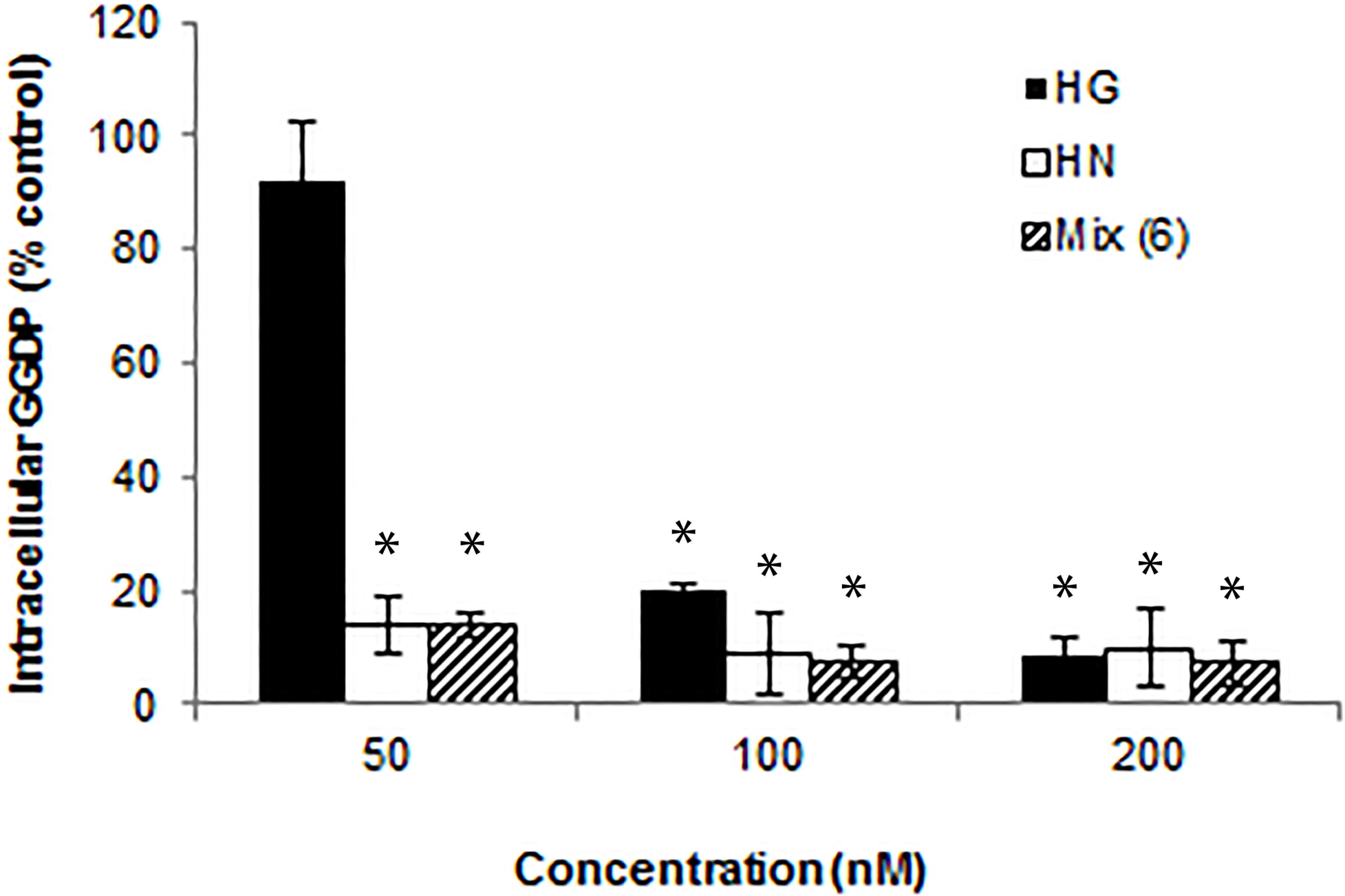
120
100
80
60
40
20
0
Intracellular GGDP (% control)
HG
HN
Mix (6)
*
50
100
200
Concentration (nM)

Figure 3

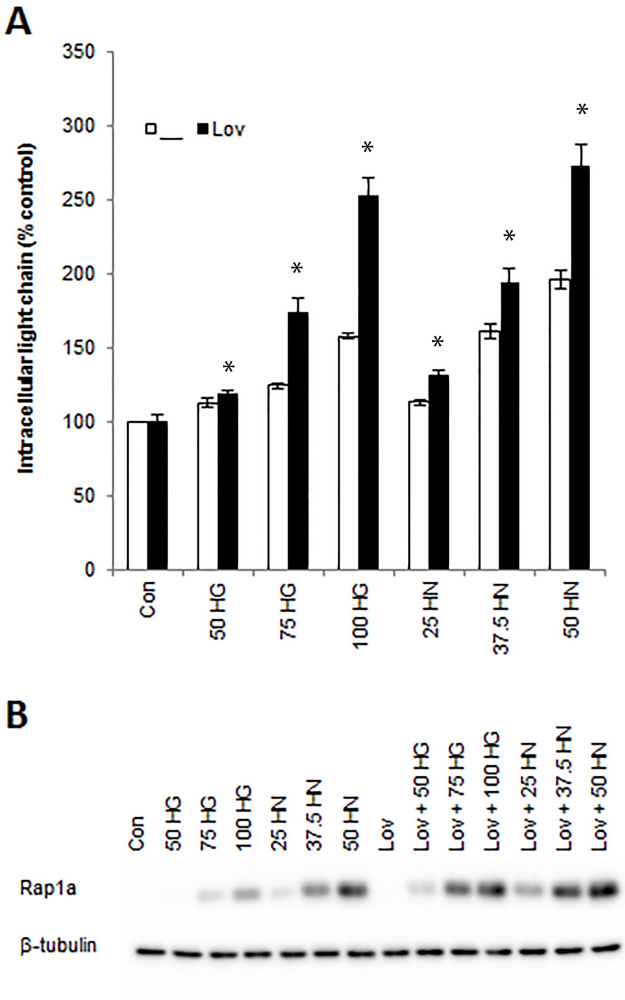
A
Intracellular light chain (% control)
350
300
250
200
150
100
50
0
Lov
*
Con
50 HG
75 HG
100 HG
25 HN
37.5 HN
50 HN
B
Con
50 HG
75 HG
100 HG
25 HN
37.5 HN
50 HN
Lov
Lov + 50 HG
Lov + 75 HG
Lov + 100 HG
Lov + 25 HN
Lov + 37.5 HN
Lov + 50 HN
Rap1a
β-tubulin

Figure 4

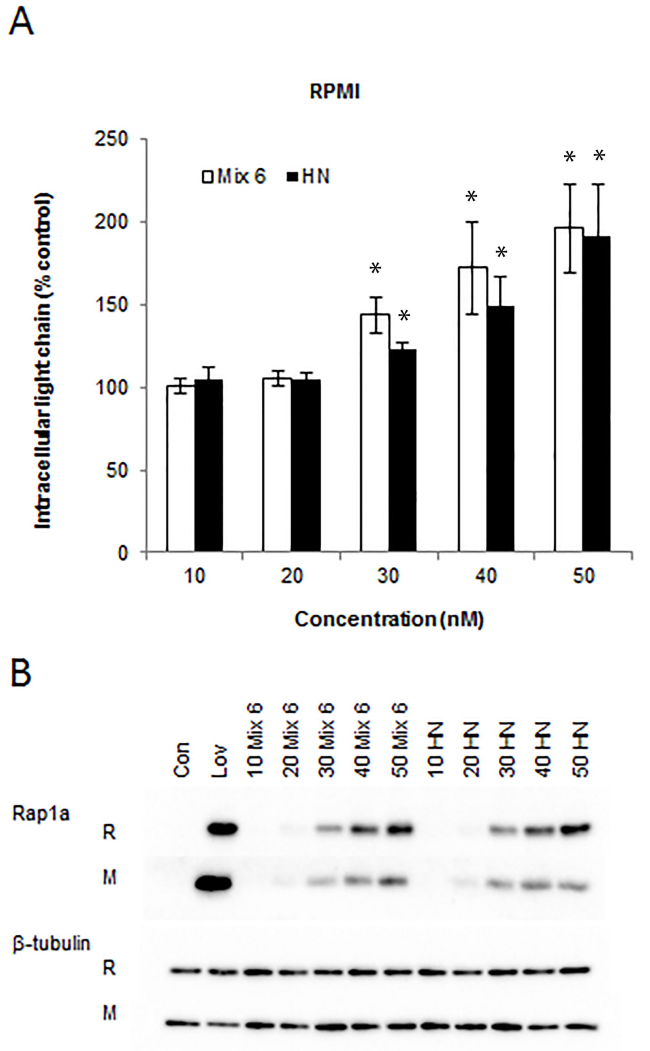
A
RPMI
Mix 6
HN
Intracellular light chain (% control)
250
200
150
100
50
0
10
20
30
40
50
Concentration (nM)
B
Con
Lov
10 Mix 6
20 Mix 6
30 Mix 6
40 Mix 6
50 Mix 6
10 HN
20 HN
30 HN
40 HN
50 HN
Rap1a
R
M
β-tubulin
R
M

Figure 5

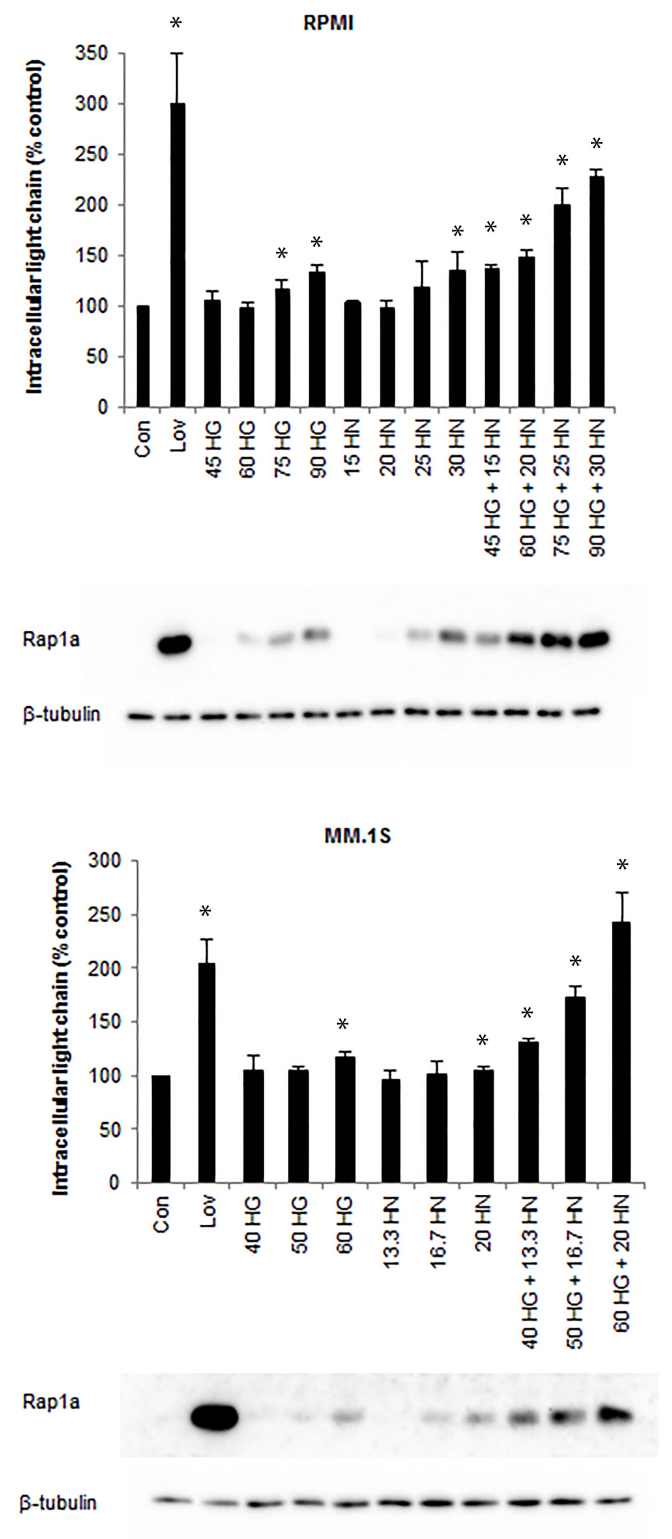
RPMI
Intracellular light chain (% control)
350
300
250
200
150
100
50
0
Con
Lov
45 HG
60 HG
75 HG
90 HG
15 HN
20 HN
25 HN
30 HN
45 HG + 15 HN
60 HG + 20 HN
75 HG + 25 HN
90 HG + 30 HN
Rap1a
β-tubulin
MM.1S
Intracellular light chain (% control)
300
250
200
150
100
50
0
Con
Lov
40 HG
50 HG
60 HG
13.3 HN
16.7 HN
20 HN
40 HG + 13.3 HN
50 HG + 16.7 HN
60 HG + 20 HN
Rap1a
β-tubulin

Figure 6

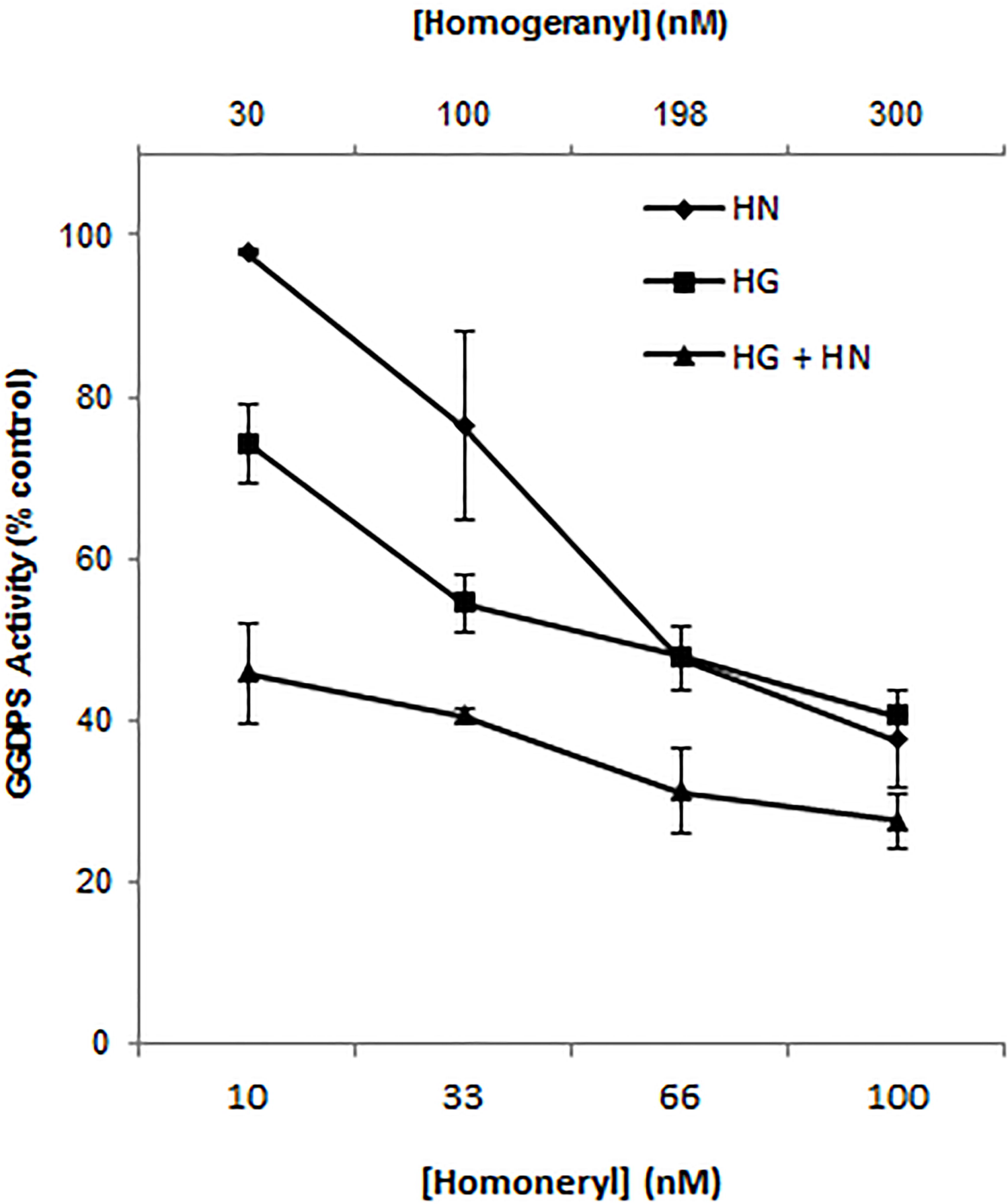
[Homogeranyl] (nM)
30
100
198
300
HN
HG
HG + HN
100
80
60
40
20
0
GGDPS Activity (% control)
10
33
66
100
[Homoneryl] (nM)

Figure 7

A

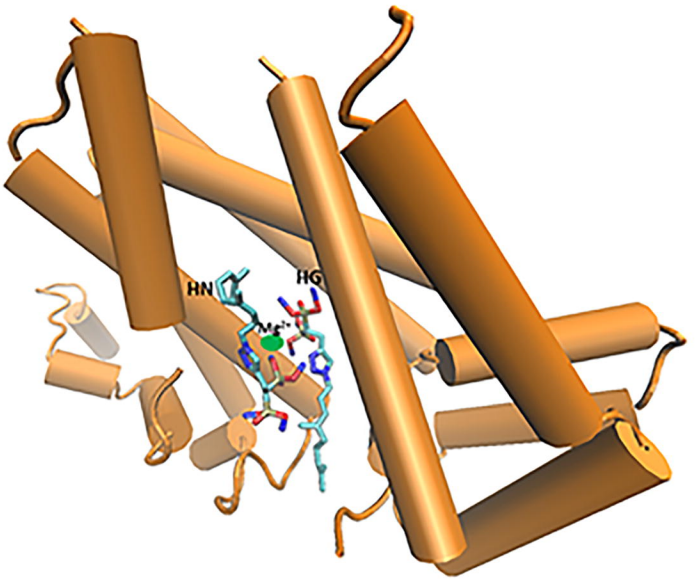
HN
HG
Mg2+

B

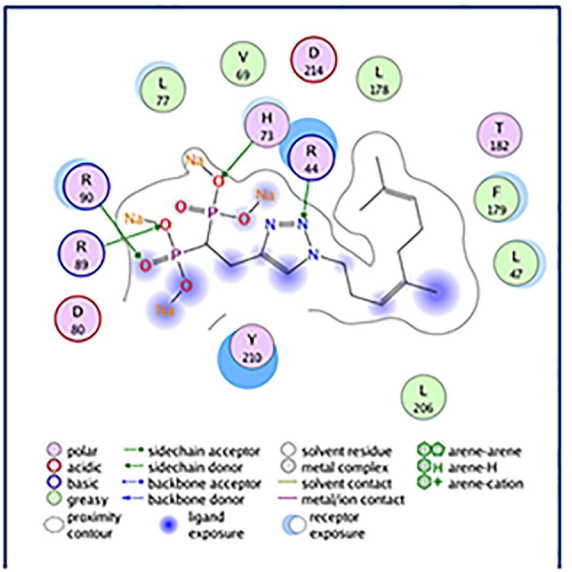
V 69
D 214
L 178
L 77
H 73
R 44
T 182
R 90
F 179
R 89
L 47
D 80
Y 210
L 206
Na
polar
acidic
basic
greasy
proximity contour
sidechain acceptor
sidechain donor
backbone acceptor
backbone donor
ligand exposure
solvent residue
metal complex
solvent contact
metal/ion contact
receptor exposure
arene-arene
arene-H
arene-cation

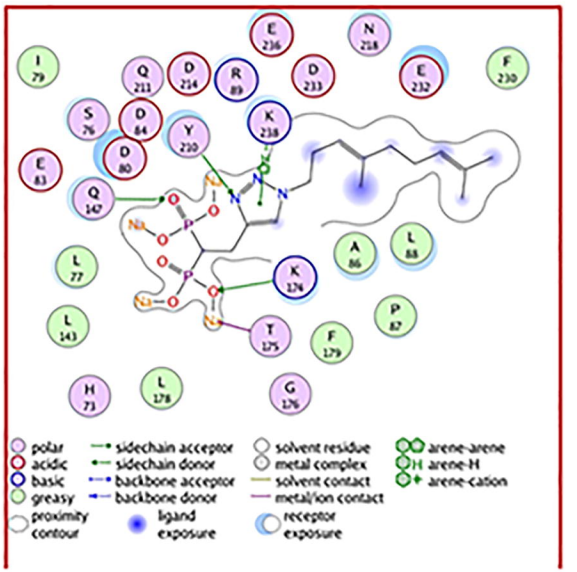
E 236
N 218
I 79
Q 211
D 214
R 89
D 233
E 232
F 230
S 76
D 84
K 238
Y 210
D 80
E 83
Q 142
L 88
A 86
L 77
K 174
L 143
P 87
T 175
F 179
H 73
L 178
G 176
Na
polar
acidic
basic
greasy
proximity contour
sidechain acceptor
sidechain donor
backbone acceptor
backbone donor
ligand exposure
solvent residue
metal complex
solvent contact
metal/ion contact
receptor exposure
arene-arene
arene-H
arene-cation

Figure 8